PCCP

RSC Publishing

PAPER

View Article Online
View Journal | View Issue

Solvatochromism of pyranine-derived photoacids†

Cite this: *Phys. Chem. Chem. Phys.*, 2013, **15**, 19893

Christian Spies,[a] Björn Finkler,[a] Nursel Acar[b] and Gregor Jung*[a]

Received 22nd July 2013,
Accepted 5th October 2013

DOI: 10.1039/c3cp53082e

www.rsc.org/pccp

Photoacidity is frequently found in aromatic alcohols where the equilibrium dissociation constant increases by some orders of magnitude upon electronic excitation. In this study we investigated the solvatochromism of a family of recently synthesized super-photoacids and their methylated counterparts based on pyrene. The chemical similarity of these molecules on the one hand and their differing photoacidity with pK_a* values between −0.8 and −3.9 on the other allow for gaining insights into the mechanisms contributing to excited-state proton transfer. Three different solvent scales, namely Lippert–Mataga, Kamlet–Taft and Catalán, were independently employed in this study and gave consistent results. We found the strongest correlation of the excited-state acidity with the dipolarity of the excited state, p_{em} ranging from −1775 cm^{-1} to −2500 cm^{-1}, and a concomitant change in the permanent dipole moment of roughly 14 Debye. Spectral changes due to varying basicity of the solvent, which probes the conjugated property of the solute, are found to be less indicative of the graduation of excited-state acidity, *i.e.* b_{em} values between −700 and −1200 cm^{-1}. The solvent acidity is the only parameter with a distinct influence on the electronic spectra of the deprotonated species. The low values of a_{em} ∼ 400 cm^{-1}, which are 3–4× smaller than a_{abs} and a_{exc}, indicate the low basicity of these species in the excited state. Triggered by semiempirical theoretical calculations, the energetic splitting between the two lowest excited states could be related to the excited-state acidity and points to alterations in the electronic mixing of locally excited and charge-transfer states, caused by the substituents. Differences between the threefold negatively charged pyranine and the new neutral photoacids are also discussed.

Introduction

Since its first description by Förster in 1949,[1] excited-state proton transfer (ESPT) has gained widespread attention.[2–5] Especially aromatic alcohols have proven to be a valuable tool to investigate the mechanism of proton transfer as they can easily be observed by absorption and fluorescence spectroscopy. Upon electronic excitation the usually weak acids undergo an increase in acidity by some orders of magnitude and are capable of transferring a proton to a suitable acceptor. The underlying reasons for the enhanced excited-state acidity have been the subject of research for more than two decades and have been reviewed many times.[2–4,6,7] Besides intramolecular charge redistribution,[8–11] the influence of the solvent on the excited-state acidity has been intensively studied.[12–15]

Photoacidity is a frequent phenomenon, and many dye molecules[16–20] and proteins[21,22] are known to release a proton in the excited state. The most intensively studied photoacids are those based on naphthol. The good UV-absorption along with their well-known electronic properties makes them well suited to investigate the important ESPT parameters, such as the nature of substituents and their positions.[8,23–29] Another paradigmatic photoacid is 8-hydroxypyrene-1,3,6-trisulfonate (HPTS, pyranine), which exhibits absorption and emission in the visible part of the electromagnetic spectrum and a high water solubility.[13,30–36]

ESPT of these photoacids to bases[32,37] or the solvent[38–40] has been reported. In most examples, the proton-accepting solvent is water because of its high polarity and unique tendency to accept and stabilize protons in a hydrogen-bonding network. Only a few molecules with an excited-state acidity constant pK_a* below zero are described, which can transfer the proton to polar, aprotic organic solvents such as dimethyl sulfoxide (DMSO).[41,42] These so-called ''super-photoacids'' may offer

[a] *Biophysical Chemistry, Saarland University, Campus, Building B2 2, D-66123 Saarbrücken, Germany. E-mail: g.jung@mx.uni-saarland.de; Fax: +49-681-302-64648; Tel: +49-681-302-64848*

[b] *Ege University, Faculty of Science, Department of Chemistry, 35100 Bornova, Izmir, Turkey*

† Electronic supplementary information (ESI) available: Detailed description of the synthesis of methylated compounds. Lippert–Mataga plots of methylated compounds. Crystal structure of compound **2b**. Correlation plots of photoacids for Kamlet–Taft and Catalán analysis. Plot of solute parameters *vs.* anion fluorescence percentage. Absorption and excitation spectra of **1a** and **1e**. Results of the theoretical calculations and molecular orbitals of **MPTA** and **MPTS**. CCDC 951707. For ESI and crystallographic data in CIF or other electronic format see DOI: 10.1039/c3cp53082e

further insights into a proton transfer mechanism in aprotic environments.[41,43–46] Further investigations were dedicated to the effects of temperature,[18,36,47–53] pressure,[54] salt concentration[37,55,56] or solvent composition[17,57,58] on the ESPT process.

The use of time-resolved spectroscopy has given many insights into the mechanism and the dynamics of proton transfer.[16,34,59–66] A convenient approach to studying the interaction between a probe and the solvent using steady-state spectroscopy is the solvatochromic analysis.[44,67–72] Absorption and emission wavelengths are collected in different media and correlated to solvent parameters from which solute properties can be deciphered. While absorption spectra are useful for the investigation of ground state properties, emission spectra contain information about the relaxed excited state. Therefore, different solvatochromic shifts of absorption and emission wavelengths indicate different interactions in both states.

Many solvatochromic scales have been developed, including empirical scales and those based on physicochemical solvent parameters.[73] An example of the latter is the Lippert–Mataga equation, which correlates the Stokes shift $\Delta\nu$ to the solvents relative permittivity ε_r and refractive index n (see the Experimental section, eqn (1)).[74–76] It is used to calculate the change of the static dipole moment of a molecule upon electronic excitation. More detailed information is obtained by empirical multi-parameter approaches that can take account of specific solute–solvent interactions, *e.g.* hydrogen bonds. Most common are those scales introduced by Kamlet and Taft[77] (eqn (2)) and, more recently, by Catalán[78] (eqn (3)). Especially the Kamlet–Taft scale has been often used to explore the important parameters of ESPT.[67,69,70,79–81] However, a systematic investigation with a series of similar photoacids that differ in their excited-state acidity is still missing.

In a parallel publication, we report and characterize a new series of highly photostable photoacids with varying photoacidity derived from pyranine.[82] Whereas their ground state pK_a values do not show much alteration, with values between 4.4 and 5.7, their excited state acidity constants pK_a* vary systematically between −0.8 and −3.9 as computed from spectroscopic data. The present paper provides insight into how these photoacids differ in their ESPT ability and describes the important solvent–solute interactions. To accomplish this task we performed a comprehensive solvatochromic analysis of six photoacids and semi-empirical AM1 calculations. To maintain the assignment of hydrogen-bond donation ability to the hydroxylic proton (moiety), a differential solvatochromism method was employed by using the methoxy derivative of the compounds (Scheme 1). Using **HPTA** and **MPTA**, the complexation constant of **HPTA** in DMSO was determined.[83]

The structure of the paper is as follows: firstly, we will describe the solvent induced changes in the absorption and emission spectra of the new photoacids. The general solvent effects as well as the photoacid effect will be discussed shortly. We will correlate these changes with various solvent parameters for acidity, basicity and dipolarity. It turns out that an increase in the static dipole moment in the excited state is the most important characteristic of excited-state acidity. Consistent results are obtained from Kamlet–Taft and Catalán analyses. Finally, theoretical calculations give preliminary hints about the molecular energetics.

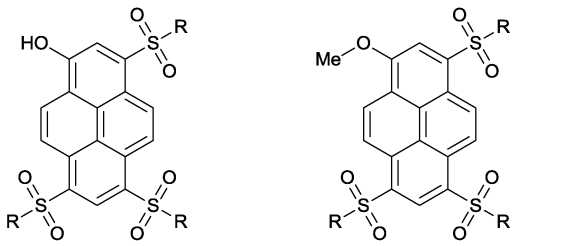

HPTS: R = -O⁻
HPTA: R = -N(CH$_3$)$_2$
1a: R = -OCH$_2$CF$_3$
1b: R = -OCH(CF$_3$)$_2$
1c: R = -N(CH$_3$)(OCH$_3$)
1d: R = -N((CH$_2$)$_2$OCH$_3$)$_2$
1e: R = -N(CH$_3$)((CH$_2$)$_2$OH)

MPTS: R = -O⁻
MPTA: R = -N(CH$_3$)$_2$
2a: R = -OCH$_2$CF$_3$
2b: R = -OCH(CF$_3$)$_2$
2c: R = -N(CH$_3$)(OCH$_3$)
2d: R = -N((CH$_2$)$_2$OCH$_3$)$_2$
2e: R = -N(CH$_3$)((CH$_2$)$_2$OH)

Scheme 1 Chemical structures of the photoacids and their methoxylated derivatives used in this study. **HPTA** and **HPTS** are known photoacids, **1a–1e** are the recently synthesized photoacids, **2a–2e** the methylated forms.

Experimental and theoretical methods

Synthesis

Compounds **2a–e** were prepared starting from **HPTS** (98%, Acros Organics) as shown in Scheme 2. By deprotonation with sodium hydroxide and reaction with methyl iodide, **HPTS** was converted into **MPTS**. The subsequent route corresponds to a synthetic pathway, which is reported elsewhere.[82] Yields were slightly lower as reported for the photoacids. A detailed description of the procedure is given in the ESI.† A crystal structure could be obtained for compound **2e**, which is shown in Fig. S1 and Table S1 (ESI†).

Spectroscopy

All solvents used for spectroscopic measurements were of spectroscopic quality if available. Moreover, they were checked for fluorescent impurities prior to use. A list of solvents used in this work as well as their solvatochromic and physical parameters are given in Table 1.

Absorption spectra were taken at micromolar concentration in quartz cuvettes (Hellma) using a Jasco V-650 spectrometer and a bandpass of 1 nm. Fluorescence spectra were measured using the Jasco FP-6500 spectrofluorimeter (wavelength accuracy ±0.5 nm). All spectra used for the solvatochromic analysis were transformed to the transition dipole moment representation, with the excitation and absorption spectra weighted with ν^{-1} and the emission with ν^{-3} as suggested by Angulo *et al.* for solvatochromic analyses.[84] We exclude chloroaliphatics and butyrolactone from any multiparameter regression as they show a deviation of the regression for all compounds.[85]

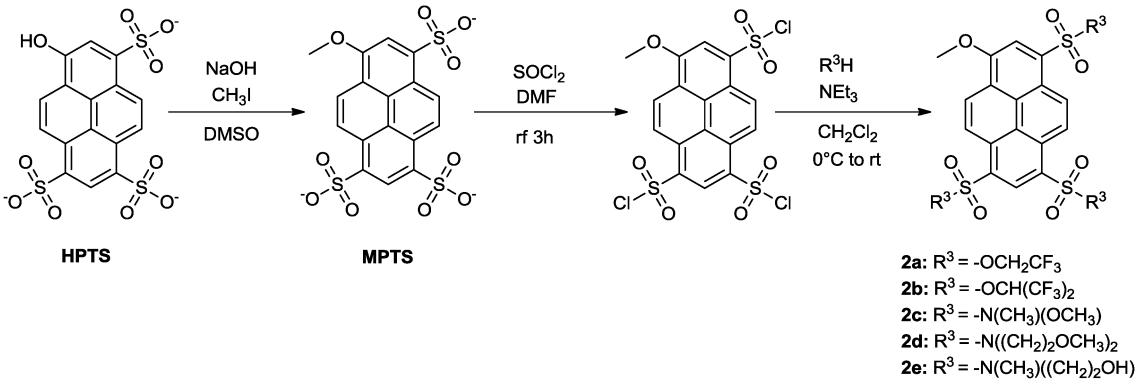

Scheme 2 Reaction scheme for the synthesis of the methylated compounds.

Table 1 Solvents and their physical (refractive index n and relative permittivity ε_r) and solvatochromic parameters (α, β, π^* and SA, SB, SP, SdP) used in this study[77,78,86]

#	Solvent	ε_r	n	α	β	π^*	SA	SB	SP	SdP
1	Cyclohexane	2.02	1.426	0	0	0	0	0.073	0.683	0
2	Tetrachloromethane	2.30	1.460	0	0	0.28	0	0.044	0.768	0
3	Bromobenzene	5.40	1.557	0	0.07	0.71	0	0.192	0.875	0.497
4	Hexane	1.89	1.375	0	0	−0.11	0	0.056	0.616	0
5	Toluene	2.38	1.497	0	0.11	0.54	0	0.128	0.782	0.284
6	Dioxane	2.21	1.422	0	0.37	0.55	0	0.444	0.737	0.312
7	Sulfolane	42.13	1.484	0	0.39	0.98	0.052	0.365	0.830	0.896
8	Propylene carbonate	64.92	1.422	0	0.4	0.83	0.106	0.341	0.746	0.942
9	Ethyl acetate	6.02	1.372	0	0.45	0.55	0	0.542	0.656	0.603
10	Diethyl ether	4.34	1.353	0	0.47	0.27	0	0.562	0.617	0.385
11	Butyrolactone	40.96	1.437	0	0.49	0.87	0.057	0.399	0.775	0.945
12	Cyclohexanone	18.30	1.451	0	0.53	0.76	0	0.482	0.766	0.745
13	Tetrahydrofuran	7.58	1.407	0	0.55	0.58	0	0.591	0.714	0.634
14	Dimethyl formamide	36.71	1.431	0	0.69	0.88	0.031	0.613	0.759	0.977
15	DMSO	46.45	1.479	0	0.76	1	0.072	0.647	0.83	1.000
16	Tetramethylurea	23.60	1.449	0	0.8	0.83	0	0.624	0.778	0.878
17	HMPT	29.60	1.459	0	1.05	0.87	0	0.813	0.744	1.1
18	Acetone	20.56	1.359	0.08	0.48	0.71	0	0.475	0.651	0.907
19	Acetonitrile	35.94	1.344	0.19	0.31	0.75	0.044	0.286	0.645	0.974
20	Nitromethane	35.87	1.382	0.22	0.06	0.85	0.078	0.236	0.71	0.954
21	Dichloromethane	8.93	1.424	0.3	0	0.82	0.04	0.178	0.761	0.769
22	Chloroform	4.81	1.446	0.44	0	0.58	0.047	0.071	0.783	0.614
23	2-Propanol	19.92	1.377	0.76	0.95	0.48	0.283	0.83	0.633	0.808
24	Ethanol	24.55	1.361	0.83	0.77	0.54	0.4	0.658	0.633	0.783
25	Ethylene glycol	37.70	1.432	0.9	0.52	0.92	0.717	0.534	0.777	0.91
26	Methanol	32.66	1.328	0.93	0.62	0.6	0.605	0.545	0.608	0.904
27	Water	78.30	1.333	1.17	0.47	1.09	1.062	0.025	0.681	0.997
28	2,2,2-Trifluoroethanol	26.53	1.300	1.51	0	0.73	0.893	0.107	0.543	0.922
29	Hexafluoro-2-propanol	16.70	1.275	1.96	0	0.65	—	—	—	—

Theoretical calculations

The Spartan08 software[87] was used to find the starting geometries of **MPTA**. This program enables us to draw the structure, optimize roughly the geometry using the MM2 force field and to generate the corresponding coordinates by conformational analysis. The ground state geometries of all of the molecules were then optimized by using B3LYP/6-31G* as implemented in Gaussian09[88] (and by the AM1 method as implemented in VAMP[89]).

Transition energy $\Delta E_{i\rightarrow j}$ corresponding to the excitation of an electron from the orbital φ_i (occupied in the ground state) to φ_j (unoccupied in the ground state) has been calculated using TD-DFT in Gaussian09 (and using PECI in VAMP).

The excited state geometries were also optimized using the AM1 method by taking into account the configuration interaction calculations (CIS = 16).

Solvatochromic scales

To calculate the change in the static dipole moment $\Delta\mu = |\mu_e - \mu_g|$ of a molecule upon electronic excitation, the Lippert–Mataga equation is used (eqn (1)).

$$hc\Delta\nu = \frac{2|\mu_e - \mu_g|^2}{4\pi\varepsilon_0 a^3}\left[\frac{\varepsilon_r - 1}{2\varepsilon_r + 1} - \frac{n^2 - 1}{2n^2 + 1}\right] = \frac{2|\mu_e - \mu_g|^2}{4\pi\varepsilon_0 a^3}\Delta f. \quad (1)$$

In this equation, $\Delta\nu$ is the Stokes shift of the molecule in Hz, n the refractive index of the medium, ε_0 and ε_r the vacuum permittivity and the relative permittivity of the medium, respectively. The parameter a is the cavity in the medium, created by the solute, whereas μ_e and μ_g are the static dipole moments of the molecule in the electronic excited and ground state, respectively.

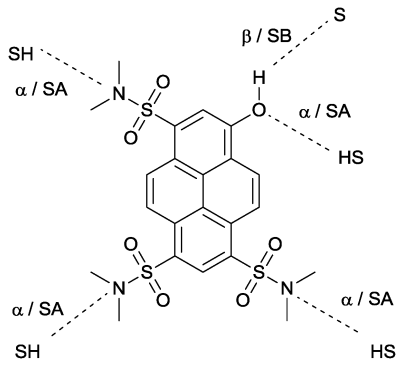

Scheme 3 Possible hydrogen bonds that the molecules can form.

To investigate the hydrogen-bond interactions of the molecules with solvents, the empirical solvent scales of Kamlet–Taft (eqn (2)) and Catalán (eqn (3)) are used. To further verify the results obtained from the Kamlet–Taft analysis, where we cancel out single parameters by appropriate molecule–solvent combinations and straightforward comparisons, we also employ the Catalán solvent scale. In contrast to the former, an unbiased multiparameter fit is applied here as a separation between the solvent parameters is not convenient. However, both scales express the value of a solvent dependent parameter ν_i, *i.e.* absorption or emission frequency, by its reference value ($\nu_{0,i}$) and a set of solute and solvent parameters. It should be mentioned, that in the Kamlet–Taft analysis the reference point is cyclohexane, whereas the Catalán scale refers to the gas phase.

$$\nu_i = \nu_{0,i} + a_i{\cdot}\alpha + b_i{\cdot}\beta + p_i{\cdot}\pi^* \quad (2)$$

$$\nu_i = \nu_{0,i} + A_i{\cdot}\mathrm{SA} + B_i{\cdot}\mathrm{SB} + p_i{\cdot}\mathrm{SdP} + Q_i{\cdot}\mathrm{SP} \quad (3)$$

The solvent parameters for the specific interactions are their acidity (*i.e.* hydrogen-bond donating ability), expressed by α and SA, respectively, as well as their basicity (or hydrogen-bond accepting ability), expressed by β and SB. The dipolarity and polarizability of the medium, just the single parameter π^* in the Kamlet–Taft relation, are considered in Catalán's equation as the factors SdP and SP, respectively. By doing so, we can also assure that the dipolarity and not a changing polarizability of the molecules is responsible for the observed shifts. Each of these solvent parameters is weighted by a solute-dependent term which, accordingly, correlates the sensitivity of the probe to the respective solvent property. The determination of these prefactors is the key step in every solvatochromic analysis as it provides the corresponding properties of the molecule under investigation, in the ground or excited state. The commonly accepted specific interactions between hydrogen (bond) donors, HB-acceptors and the molecules under investigation are shown in Scheme 3.

Results and discussion

The fluorescence spectra of the six photoacids in DMSO are shown in Fig. 1(a). All spectra are normalized to the anion emission peak.

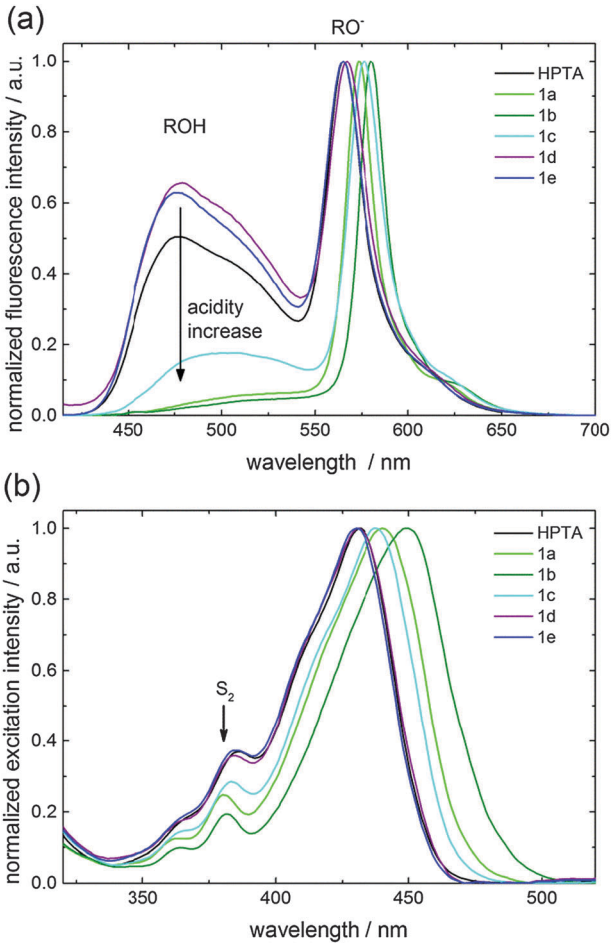

Fig. 1 (a) Normalized fluorescence emission spectra of the investigated photoacids in DMSO (λ_{ex} = 400 nm). The intensity of the acid band decreases with increasing photoacidity. (b) Normalized excitation spectra of the photoacids (λ_{em} = 600 nm). The S_2-state is assigned according to ref. 10.

The solvent DMSO is a vivid choice here because the pK_a*-values are in a range where all photoacids can undergo ESPT in this medium to a varying extent. The strength of photoacidity can easily be discussed with respect to this plot (Fig. 1a), as with increasing photoacidity the amount of acid fluorescence at λ = 450–550 nm decreases (eqn (4)).

$$\mathrm{p}K_a^* \propto \frac{I_{ROH}}{I_{RO^-}} \quad (4)$$

It should be mentioned that we rely on the definition of the thermodynamic parameter K_a* by kinetic parameters, *i.e.* the rate constant of the process, k_{ESPT} divided by the rate constant for geminate recombination, as observed in the steady state spectra. However, as the fluorescence lifetime and the fluorescence quantum yields of all anionic compounds are very similar and proton diffusion in DMSO was not detected so far,[82] our approach to classify the strength of photoacidity on the basis of the emission spectrum (eqn (4)) seems valid and more sensitive here.

The strongest photoacid is compound **1b** with hexafluorinated isopropyl substituents as the most electron withdrawing

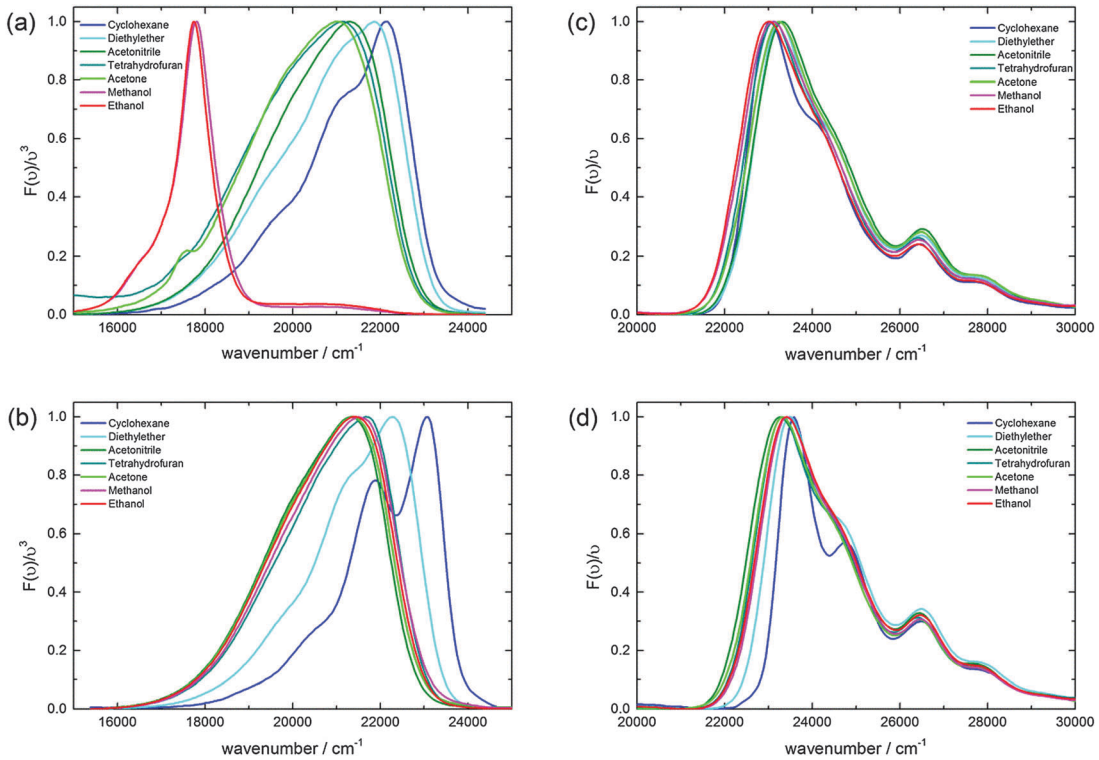

Fig. 2 Normalized fluorescence emission spectra of (a) **1a** and (b) **2a** in several solvents of differing polarity. The corresponding excitation spectra of **1a** and **2a** in the same solvents are shown in (c) and (d), respectively.

group within this series. A high photoacidity is accompanied by a slight bathochromic shift of the anion emission wavelength, $\lambda_{em,max}(RO^-)$. Concomitantly, the wavelength range of the acid emission also shifts to the red as the extent of ESPT increases. The corresponding excitation spectra are displayed in Fig. 1b. Also the excitation maxima undergo a bathochromic shift with increasing photoacidity. Most interestingly, the S_2 band[10] at $\lambda_{ex} \approx 380$ nm is hardly affected, only the S_2 state of the strongest photoacids **1a** and **1b** displays a slight hypsochromic shift.

Besides these general effects, some phenomenological solvent effects are exemplified in Fig. 2, where the excitation and emission spectra of **1a** and its methylated counterpart **2a** in different solvents are shown. Similar results are obtained for the other photoacids emphasizing the generality of these experimental findings.

Both emission and excitation spectra exhibit a bathochromic shift in solvents with higher polarity. This shift is more pronounced in emission than in excitation, which gives a first hint that the molecule has a higher polarity in the excited state than in its ground state. The photoacid and its methylated derivative behave similarly. This is to be expected, as the electronic effect of a proton and a methyl group is not very different, which is the basis for a differential solvatochromism approach (see next section).[70,80] Another effect observed in Fig. 2 is the clear vibronic structure seen in nonpolar cyclohexane with a Franck–Condon progression of $\bar{\nu} \approx 1160$ cm^{-1} for emission of **1a** and **2a**. This value is observed both in emission and excitation, although the latter is less obvious due to the overlap with the second electronic excited state at $\bar{\nu}_{exc} = 26\,525$ cm^{-1}. A similar progression is found for all other investigated compounds as well. We conclude, therefore, from these coincidences and the wavenumber range that this progression reflects a bond-length alteration in the *O*–pyrene distance but not in the sulfon-substituents. In solvents with a higher polarity, the vibronic structure is blurred out. The effect of hydrogen bonding ability and polarity of the solvent on the vibronic structure of **HPTS** has already been discussed.[12,13,33]

From Fig. 1 it is already clear that all photoacids studied in this contribution (except the previously investigated[80] **HPTS**) undergo ESPT in DMSO. Further solvents in which ESPT could be observed are the aprotic butyrolactone, dimethyl formamide, tetramethylurea and, to a minor extent, acetone. Furthermore, protic solvents such as methanol, ethanol and 2-propanol are also suitable media to observe ESPT of these photoacids. From these general considerations we can summarize that the photoacids and their corresponding methoxylated counterparts show in principle a similar solvatochromic behavior towards solvent polarity. The main difference is the occurrence of ESPT in protic and very basic, aprotic solvents.

Based on the different solvent dependence of excitation and emission spectra we analyzed the Stokes shift of the photoacids in terms of the Lippert–Mataga equation. To avoid any influence of hydrogen bonding from the hydroxyl group we used the methylated counterparts of the photoacids. As we have shown above, their electronic properties are very similar to those of the acids. In contrast to our findings for **MPTS**,[80] a clear

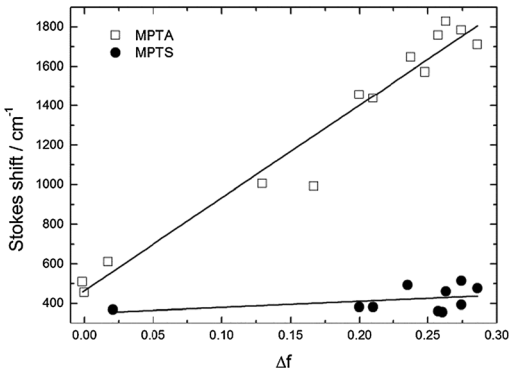

Fig. 3 Lippert–Mataga plot of **MPTA** and **MPTS** for non-acidic solvents. Correlation coefficients are R^2 = 0.96 and R^2 = 0.05, respectively. The slope of the **MPTA** regression curve is 4690 (±285) cm^{-1}. The values and plots of the other compounds as well as a correlation of the slope with the photoacidity are given in Fig. S2 and Table S2 (ESI†).

dependence according to eqn (1) is found for **MPTA** in non-protic solvents (Fig. 3).

As for **MPTA**, a similar strong dependence is seen with the compounds **2a–2e**, where the slope correlates with the photoacidity (Fig. S2, ESI†). Using a solvent excluded volume a^3 of 414 Å^3 determined using Chem3D Pro (CambridgeSoft) for the molecule, a change of the permanent dipole moment $\Delta\mu \approx 14$ D is calculated for **MPTA**. The value of the molecular volume given here is comparable to those listed for molecules of similar size.[90] Despite the rough estimate of the molecular volume, a huge change in the dipole moment is evident for all newly synthesized compounds. Our findings are in agreement with the models of a significant charge transfer (CT) occurring before the proton transfer step, resulting in the high photoacidity of aromatic alcohols. Although it is still unclear whether a larger CT is happening on the acid or the base side,[2,5] these results support a CT before any proton transfer. It has been discussed that a slow charge transfer might occur in all neutral photoacids, in contrast to cationic photoacids.[11] The lack of a Lippert–Mataga correlation seen with **HPTS** may be attributed to the three full negative charges on the sulfonate-substituents, which are supposed to obscure the transfer of partial charges.[61] The stabilizing effect of the solvent continuum is assumed to be the main contribution of the relative acidity increase $\Delta pK_a = pK_a - pK_a^*$ when going from **HPTS** to the here presented photoacids. Whereas the latter compounds undergo changes by up to 8 pK_a-units upon excitation, pyranine shows only an increase by 6 orders of magnitude, *i.e.* pK_a = 7.4 is shifted to pK_a^* = 1.4.[61]

However, a large CT in the excited state should also be indicated in a Kamlet–Taft analysis (eqn (2)) in the form of a larger value of p_{em} compared to p_{abs}. A plot of the respective spectroscopic maxima of **MPTA** and compounds **2a–2e** is shown in Fig. 4. Only non-acidic solvents (α = 0) were used for this plot and, as there are no acidic protons identified in those molecules, also b_i = 0. Therefore, a linear dependence on

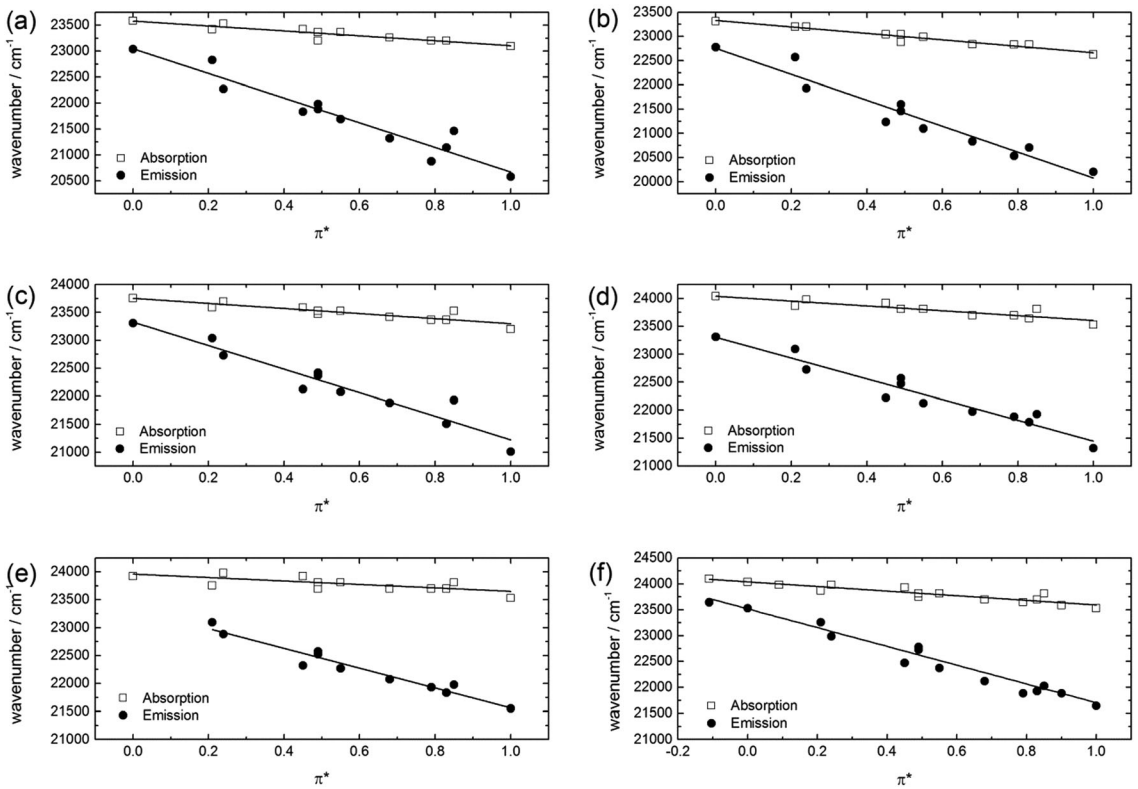

Fig. 4 Absorption (squares) and emission (circles) frequencies of the methylated photoacids in solvents of increasing polarity. (a) **2a**, (b) **2b**, (c) **2c**, (d) **2d**, (e) **2e**, (f) **MPTA**.

Table 2 Kamlet–Taft parameters p_{abs} and p_{em} of the methylated compounds. Standard errors are in parentheses, R^2 is the correlation coefficient. All values are given in cm^{-1}

Compound	$\nu_{0,abs}$	p_{abs}	R^2	$\nu_{0,em}$	p_{em}	R^2
MPTA	24 040 (30)	−445 (50)	0.84	23 500 (60)	−1870 (100)	0.96
2a	23 550 (55)	−475 (65)	0.69	23 045 (130)	−2375 (215)	0.92
2b	23 300 (70)	−670 (55)	0.70	22 700 (160)	−2500 (260)	0.89
2c	23 750 (45)	−455 (75)	0.80	23 325 (120)	−2110 (200)	0.92
2d	24 045 (40)	−435 (65)	0.85	23 300 (95)	−1855 (155)	0.93
2e	23 960 (60)	−310 (95)	0.55	23 340 (90)	−1775 (130)	0.94

solely π^* is expected, which is also observed. The results of this analysis are listed in Table 2.

If protic solvents ($\alpha \neq 0$) are also taken into account, the quality of the regression was improved upon considering an almost negligible dependence on a_{em} in emission ($a_{em} \approx -200\ cm^{-1}$) for all compounds (Table S3, ESI†). We attribute this finding to a small interaction of proton donors with the substituents on the pyrene core or, less likely, to an interaction with the methoxy-moiety. For **MPTA**, our values are close to those given by Pines for the emission frequencies although this author did not exclude a β-dependence *a priori*.[5]

All methoxy derivatives exhibit an approximately fourfold increase in p, thus fulfilling the expectation $p_{em} > p_{abs}$. Furthermore, we found that both values for p_{abs} and, especially, p_{em} increase with a higher photoacidity of the corresponding free acid as defined in Fig. 1. A plot of the acidity according to eqn (4) *vs.* the p_{em} values obtained from the above analysis is shown in Fig. 5.

Comparison was done with the unbiased and independent analysis according to the Catalán-solvent scale. Thus, the methylated compounds could all be fitted by a three-parameter fit, including solvent polarizability SP, solvent acidity SA and solvent dipolarity SdP. Those parameters that were found to be significant ($p < 0.02$) are listed in Table S4 (ESI†). However, any dependence on SB was excluded as no acidic protons are present in these molecules.

All molecules show only a minor dependency on solvent polarity (SdP) in the ground state, which strongly increases in emission.

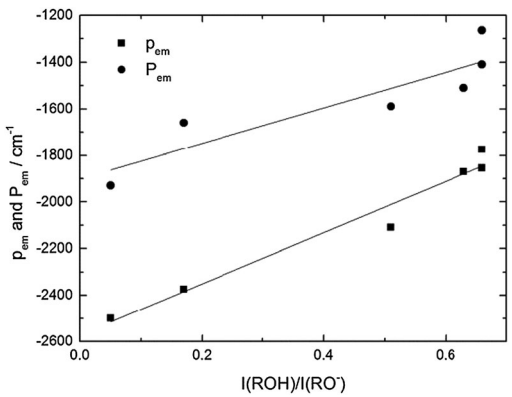

Fig. 5 Correlation of the photoacidity according to eqn (4) with p_{em} ($R^2 = 0.96$) and P_{em} ($R^2 = 0.77$) as obtained from fitting of methylated compounds. Thus, the spectroscopic properties of the methylated derivatives can be connected to the reactivity of the parent molecules.

As found in the Kamlet–Taft analysis above (Table 2), a systematic increase of the molecules' dipolarity in the excited-state (parameter P_{em}) with higher photoacidity of the corresponding photoacid is noticed (Fig. 5). Also the hydrogen-bond donated by a solvent molecule becomes more important in the excited state, parameter A_{em}. However, the molecules **2a** and **2b** with the fluorinated substituents completely lack sensitivity towards SA in the ground state as seen from $A_{abs} = 0$, which may be due to a repulsive effect of the fluorine atoms which hinders the formation of a hydrogen bond with the oxygen atom on the substituents or which might reflect hydrogen-bonds to the electron lone pair of the nitrogen of the sulfonamide bearing photoacids (Scheme 3). Furthermore, solvent polarizability is of importance for the solvatochromism of these dyes. In the ground state this is the most distinct solvatochromic factor, which is understandable as neither a distinct dipole moment nor basic sites exist. In the excited state, polarizability and dipolarity are of about equal influence. The slightly higher stabilization due to the solvent polarizability in the excited state can be related to the experimental observation that the optical spectra of neutral compounds are blue-shifted when transferred from solution to the gas phase.[91] Besides this additional information, the overall agreement between the Kamlet–Taft and Catalán analyses of the methylated compounds is large. As can be seen by comparison of Tables S3 and S4 (ESI†), correlation coefficients R^2 are better for the Catalán analysis, which is due to the importance of solvent polarizability.

In the next step we transfer these findings to the analysis of the free photoacids. We start again with the Kamlet–Taft scale and use a differential solvatochromism approach[70,80] here as the electronic properties of methylated compounds and photoacids are very similar. Furthermore, it facilitates the assignment of the β-dependence to the hydroxyl proton. As in this formalism the p_i values of photoacid and methylated compound are the same, *i.e.* p_i(**MPTA**) = p_i(**HPTA**), eqn (5) is used to determine the b_i values.

$$\nu_i(\mathbf{HPTA}) - (\nu_{i,0}(\mathbf{MPTA}) + p_i(\mathbf{MPTA})\cdot\pi^*) = \Delta\nu_{0,i} + b_i(\mathbf{HPTA})\cdot\beta \quad (5)$$

The corresponding values for absorption and emission are depicted in Table 3. The corresponding correlation curves are shown in Fig. S3 in the ESI.† For most of the molecules besides **HPTA**, only modest R^2 values are obtained for these correlations. One reason for this lies in the broadening of the peaks with increasing solvent polarity (Fig. 2) and, in the case of emission, increasing proton transfer efficiency. Another reason

Table 3 Kamlet–Taft parameters b_{abs} and b_{em} of the photoacids. Standard errors are in parentheses, R^2 is the correlation coefficient for the plots in Fig. S3 (ESI). All values are given in cm^{-1}

Compound	b_{abs}	R^2	b_{em}	R^2
HPTA	−560 (90)	0.95	−980 (190)	0.89
1a	−450 (150)	0.76	−935 (330)	0.62
1b	−645 (150)	0.83	−1200 (420)	0.66
1c	−520 (105)	0.79	−700 (210)	0.72
1d	−400 (100)	0.66	−825 (125)	0.84
1e	−330 (120)	0.58	−820 (155)	0.80

could be some residual, yet overlooked CH-acidity of the methyl group which serves as reference in eqn (5). Moreover, good solubility of the various compounds in common solvents minimizes the number of employable solvents.

As observed before for the solutes dipole moment ($p_{em} > p_{abs}$), the strength of the hydrogen bond from the hydroxyl group to a solvent molecule also increases upon excitation and hence, $|b_{em}| > |b_{abs}|$. This is a general observation within all the photoacids investigated in the literature and a hint that the reason for photoacidity is partially on the acid side.[5,70,79] A slight dependence of b_{em} on the photoacidity of the molecules can be deciphered, but is not as distinct as expected from the mentioned studies. Whereas the parameter p increased 4–5 times upon electronic excitation, b is just increasing by a factor of about two. Moreover, the variation of b_{em} with the acidity is less pronounced than that of p_{em}, as shown in Fig. S4, ESI.† Concerning the high photoacidity of the investigated photoacids, the parameter b_{em} is also surprisingly small compared to those given in the literature for similar compounds, **HPTS**[3,81] and (cyano-)naphthols.[70,79] On the other hand, the values given here are in agreement with our previous findings for pyranine, with b_{em}(**HPTS**) = 560 cm^{-1}, indicating its much lower photoacidity.[80]

We also compare the results of the free photoacids with the Catalán solvent scale. Again, multi-parameter fits were performed and compared to the results of the methylated compounds. By doing so we get an unbiased picture of their solvatochromism as the analysis with the Kamlet–Taft scale was somehow driven by chemical intuition (eqn (5)). The parameters obtained from the Catalán analysis of the free photoacids are shown in Table S5 (ESI†) and the corresponding correlation curves are displayed in Fig. S5 (ESI†). Here, higher correlation coefficients are found than for the Kamlet–Taft analysis as the solvent polarizability is considered.

For the ground state, a rough agreement between the parameters Q_{abs} and P_{abs} of methylated and free photoacids is found, indicating the validity of the multi-parameter approach. The multi-parameter fits of the emission frequencies of the photoacids show a lesser influence of the solvent's dipolarity compared to their methylated counterparts. However, fixing P_{em} to those values of their methylated analogs does not change the values for the basicity significantly (data not shown). Protic solvents become slightly more important for the hydroxylic compounds, which may be due to an additional larger interaction of the hydroxyl group than the methoxy group. This larger interaction amounts to less than 200 cm^{-1} but is observed for all compounds. The main stabilization of the free acids in the electronic ground state according to the Catalán analysis, beyond the solvent's polarizability comes from its basicity. This is in rough agreement with the Kamlet–Taft analysis which shows an equal importance of π^* and β for spectral changes in the electronic ground state.

Upon excitation of the molecules, basicity of the solvent becomes more important by a factor of up to two. As in the Kamlet–Taft analysis (parameter b_{em}), no distinct correlation of B_{em} with the photoacidity of the compounds is observed. Furthermore, the parameter for solvent acidity increases by a factor of about two, $A_{em} \approx 2A_{abs}$, as seen for the methylated compounds (Table S3, ESI†).

From the above considerations we find a significant dependence of a solvatochromic parameter on the photoacidity of the photoacids only for the dipolarity of the solvent. Solvent basicity as well as polarizability also plays a role in the solvatochromic behavior but, from our data, no distinct correlation with the photoacidity could be extracted.

As not only the photoacid is of importance in ESPT reactions but also the product of the proton transfer, we investigated the solvatochromism of the corresponding anion, as well. It can be fully described by an α-dependence (Fig. 6 and Table 4) in a Kamlet–Taft analysis. Neither the polarity nor the basicity of the solvent has an obvious influence on absorption or emission wavelengths. It is also worth noting that the Franck–Condon progression, clearly visible for the acids and their methylated counterparts, is almost completely lacking.

These findings are in agreement with those results obtained for other photoacids based on naphthol[44,70] and **HPTS**.[80] Both absorption and emission frequencies are blue-shifted with increasing hydrogen-bond donating strength. The effect is much more pronounced in the ground state, in agreement with a more negatively charged oxygen atom in the ground state. In the excited state, charge density is presumably transferred from the oxygen towards the ring system and hence, the blue-shift is significantly smaller for emission frequencies, *i.e.* α_{abs} is about 3–4 times larger than α_{em}.

Nevertheless, no stringent correlation of the a_{exc}-values with the acidity of the corresponding photoacid is obtained, just slightly smaller values are determined for **1a** and **1b**. The values for the excited state a_{em} do not change at all for all photoacids investigated within the error margins and might also reflect interactions with the sulfonamide-residues, similar to those observed for the methylated compounds (Table 2). The decrease of a_{em} compared to a_{exc} because of the lower basicity in the excited state has also been noticed in a study of β-naphthol by Solntsev, Huppert and Agmon.[70] They found a_{exc} = 3100 cm^{-1} and a_{em} = 1770 cm^{-1}, which is two to three times larger than the values given here. However, the photoacidity of β-naphthol is much weaker (pK_a^* = 2.8) and those findings support our observation that a_{exc} is lowered with higher photoacidity. Furthermore, in the same paper they predicted this trend by comparison with the 5-cyano derivative of β-naphthol, which is supported by our results. The photoacidity of this molecule is very

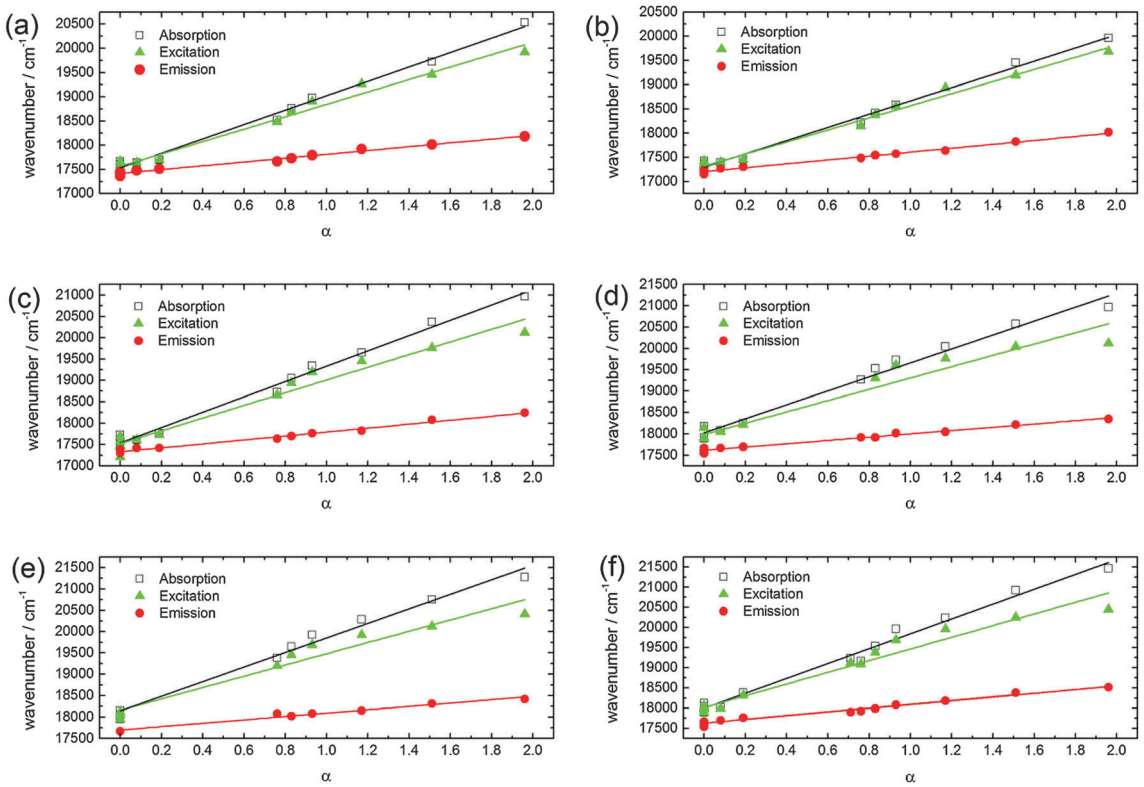

Fig. 6 Absorption (open squares), excitation (triangles) and emission (circles) frequencies of deprotonated photoacids in solvents of increasing acidity. (a) **1a**, (b) **1b**, (c) **1c**, (d) **1d**, (e) **1e**, (f) **HPTA**. The reproducible difference in the slope of excitation and absorption might point to the coexistence of a non-fluorescent complex[92] and will not be discussed further in the present manuscript. Absorption and excitation spectra of two compounds are shown in Fig. S6 (ESI†).

Table 4 Kamlet–Taft parameters of the deprotonated photoacids. Standard errors are in parentheses, R^2 is the correlation coefficient. All values are given in cm^{-1}

Compound	$\nu_{0,abs}$	a_{abs}	R^2	$\nu_{0,exc}$	a_{exc}	R^2	$\nu_{0,em}$	a_{em}	R^2
HPTA	18 000 (45)	1845 (55)	0.97	18 015 (60)	1450 (75)	0.96	17 630 (20)	460 (20)	0.98
1a	17 535 (30)	1485 (35)	0.99	17 565 (35)	1280 (45)	0.98	17 415 (10)	395 (15)	0.98
1b	17 300 (30)	1365 (35)	0.99	17 315 (30)	1250 (35)	0.99	17 205 (10)	405 (10)	0.99
1c	17 540 (45)	1790 (50)	0.99	17 530 (70)	1485 (80)	0.96	17 335 (15)	460 (20)	0.98
1d	18 025 (65)	1630 (75)	0.98	17 985 (110)	1320 (120)	0.93	17 615 (15)	385 (15)	0.98
1e	18 145 (65)	1705 (70)	0.99	18 160 (115)	1320 (110)	0.95	17 700 (30)	395 (25)	0.97

similar to **HPTA** in terms of pK_a* but they give a_{em} = 1100 cm^{-1} for its anion emission frequency, which is roughly twice as much as the value for **HPTA** (Table 4). We attribute this finding to the much better resonance stabilization of the anion in pyrene-based systems compared to naphtholates.

The values found for **HPTS** in our previous study[80] are in disagreement with the above considerations. Although it is a weaker photoacid than the molecules studied here, both a_{exc} and a_{em} of **HPTS** (a_{exc} = 780 cm^{-1}, a_{em} = 240 cm^{-1}) are smaller than those for the stronger acids. We interpret this finding with the following: **HPTS** has three negatively charged substituents which can act as strong hydrogen-bond acceptors, which may lower the energy of the electronic states as do hydrogen-bond donors for the neutral acids (see Table 2). The interaction of these additional charges is supposed to interfere with any effect of the deprotonated hydroxyl group and, thus, may lower the a_t-values. This explanation is corroborated by the low correlation coefficients obtained for **HPTS** compared to the neutral photoacids.

The results of the multiparameter fitting to Catalán parameters of the photoreaction's products are shown in Table S6 (ESI†). Besides the influence of the solvent's acidity already noticed in the Kamlet–Taft analysis, which is similarly reduced by a factor of ~4 in the excited state, the solvent polarizability also contributes to the solvatochromism of the anion, whereas dipolarity and basicity of the solvent do not influence the transition wavelengths of all compounds. The A_{abs} values are not found to change much concerning the large error margins. For all compounds we find $Q_{abs} > Q_{em}$ indicating a higher polarizability in the ground state. We interpret this finding by a partial transfer of electronic charge from the oxygen atom to the pyrene core upon excitation. The shift of the outer, non-bonding electrons to the inner part of the molecule presumably leads to a reduced polarizability. A similar explanation has been

made earlier for fluorescent proteins using two-photon absorption[93] and is also exemplified by the red-shifted electronic spectra of other anionic compounds when transferred to the gas phase.[94]

In summary, our results from the solvatochromic analysis suggest that the stronger photoacidity change in our pyrene photoacids when compared to **HPTS** is based on the dipolarity of the excited state. Neither a dramatic increase of the hydrogen-bond strength from the hydroxyl group to a solvent molecule, nor that from the solvent to the photoproduct state, nor any evidence for an energy transfer from electronic energy to the OH-stretch, as reported by others,[95] can explain the high photoacidity of the pyranine derivatives.

According to our solvatochromic studies, the clue to photoacidity lies in the charge-transfer but it is unclear at this stage of the study whether CT is mandatory for ESPT as **HPTS** can also undergo ESPT.

To learn more about the electron distribution and charge transfer state after excitation we investigated prototypical **MPTA** and **MPTS** using semiempirical CIS calculations. Although these calculations basically serve as a first hint, they are nevertheless useful to get insights into the nature of excited states. The properties of the calculated states for **MPTA** in the solvent acetonitrile are shown in Table S7 (ESI†) and the corresponding molecular orbitals are displayed in Fig. S7 (ESI†). From these data, states containing different amounts of localized excitation (LE) and charge transfer (CT) character can be identified. The HOMO–LUMO transition shows no strong CT but basically locally excited states on the pyrene core, although a decrease of electron density on the methoxy oxygen can be detected. We find a substantial amount of CT in the states S_3, S_4 and S_5 coming mainly from charge migration from the sulfonamide substituents to the pyrene core ($\Delta\mu \approx$ 6–8 D). This is an unexpected result when one keeps in mind that the stronger photoacids were produced by introducing stronger electron-withdrawing groups to the pyrene core compared to **HPTA**. Furthermore, the empirical data from the present solvatochromism study hint to a CT from the ring to the substituents as the reason for the increased photoacidity. It is interesting to note that the calculations carried out for **MPTS** showed no significant CT in the first seven excited states (Fig. S8 and Table S8, ESI†). This result can point to differences in the origin of photoacidity of the known pyrene-derived photoacids, as was already pointed out before.[9]

The polar states of **MPTA**, which were also found in gas phase calculations, have a much lower energy in acetonitrile compared to the energy values *in vacuo* (Fig. 7). Concerning the low accuracy of the method in absolute energy values, it might be that those states are closer in energy than the calculations imply, leading to a major role of the charge transfer states for the photophysics of pyrene derivatives. Even a state reversal, as deciphered for **HPTS** by experiments,[10,13,33] could be imagined and would fit to absorption data (see below). As no CT is evident from our calculations for **MPTS**, no inversion of states is found for this compound.

Furthermore, a transition involving a CT from the methoxy group to the ring system (H − 6 to L + 5) is found to contribute around 10% to the excited-state configuration in the S_1 state.

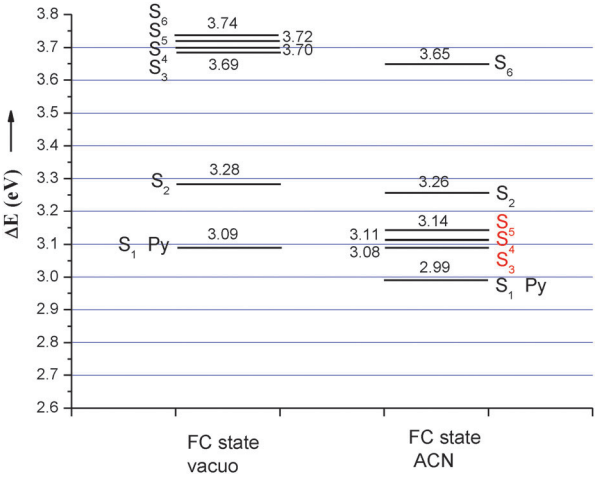

Fig. 7 Comparison of excitation energies in the Franck–Condon state *in vacuo* and acetonitrile (ACN) for **MPTA**, respectively.

This shows a smaller charge density on the oxygen atom in the excited state, an argument often used to account for the high photoacidity of these systems. More extensive and accurate calculations as well as the use of explicit solvent models are necessary to completely understand the charge redistribution processes in this system.

From these preliminary computations, it seems that the spectroscopically observable second excited state, *i.e.* the state triple S_3–S_5 from the semiempirical calculations, could be significant for the photoacidity. We therefore investigated the energetics of the S_2-state as well (Fig. 2c and d).

It turns out that the energy difference between the first and second excited electronic state increases with higher photoacidity, whereas the absolute position of the second excited state is almost unaffected by the substituents. This is shown in Table 5 and Fig. 8a for the values obtained in DMSO. However, the same trend is displayed in other solvents, *e.g.* diethyl ether, ethanol and cyclohexane (data not shown). Furthermore, the weaker π^* dependence of the S_0–S_2 transition compared to the lowest energetic transition (Fig. 8b) contradicts a dominant CT-character of the spectroscopic S_2-state.

There are, at least, two possible interpretations of how the S_2-state triplet found in QC-calculations can influence the photoacidity:

(1) These states move below the S_1 state during solvation due to solvent relaxation, *i.e.* level crossing, and behave as a

Table 5 Energy difference between first and second excited states as observed in DMSO. All values are given in cm^{-1}

Compound	$\Delta E(S_2 - S_1)$
HPTS	2236
HPTA	2786
1a	3520
1b	3857
1c	3277
1d	2772
1e	2718

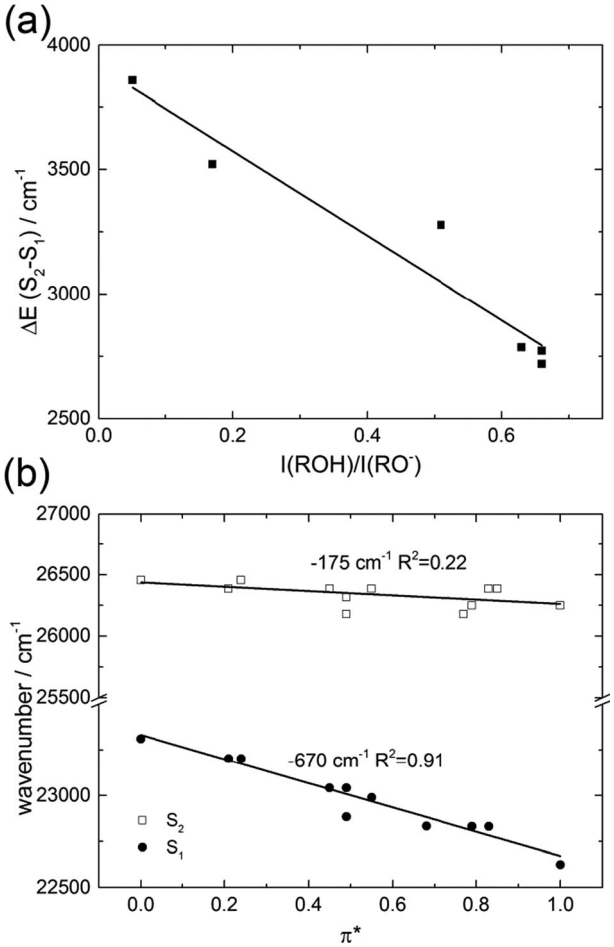

Fig. 8 (a) Correlation of the energy difference between S_1 and S_2 with the photoacidity definition according to eqn (4) (R^2 = 0.91). (b) Correlation of S_1 and S_2 absorption maxima with solvent polarity parameter π^*.

dark state with a relatively low oscillator strength. Consequently, ESPT then only occurs by thermal depopulation of these polar states during the fluorescence lifetime of the molecule. This model could explain why **HPTS** undergoes ESPT without a change in the dipole moment as such stabilization by the solvent is not mandatory for exhibiting ESPT. Photoacidity and intramolecular charge-transfer would be competitive processes in the excited state. However, this explanation is against the accepted model of CT preceding the ESPT step. Secondly, a better stabilization of the dark CT states by polar solvents is in contrast with the experimental findings as ESPT is faster in polar solvents.

(2) A real mixing with the S_1 state partially transfers CT-character to the first excited state and this mixing is reduced with increasing $\Delta E(S_2 - S_1)$. As the calculated CT in these states is a transfer of electron density from the side-groups to the ring, they are probably counteracting the ESPT process. Such heavy mixing of the lowest energy levels was also pointed out before for **HPTS**[12] and in a recent time-resolved study of 1-naphthol and 2-naphthol.[96] This model can explain why **HPTS**, having the lowest energy gap $\Delta E(S_2 - S_1)$, is a weaker photoacid and shows that side-chain modifications are a convenient way to manipulate the mixing of states.

A definite answer to the different possibilities can be hardly made on the basis of our experiments, but the solvatochromic analysis indicates that the S_1 state reached in absorption is more polar than the S_2 (see Fig. 2 and 8b), whereas the emissive state is of even more CT character. Further research should focus on both time-resolved experiments and theoretical calculations to elaborate the nature and dynamics of the first few excited-states of the here presented photoacids.

Conclusions

We investigated the solvatochromic behavior of several photoacids based on pyrene as well as their methylated derivatives. Different models were exploited to find a correlation between photoacidity and molecular properties. Lippert–Mataga plots reveal a distinct change in the static dipole moment upon excitation. The analyses according to Kamlet–Taft and Catalán, which also take into account specific hydrogen bonding interactions, verify that a high dipole is predominantly formed in the excited state. Moreover, both solvent scales provide a strong correlation of the photoacidity with the amount of intramolecular charge transfer in the excited state. This charge redistribution is not observed for HPTS, which presumably results from the shielding by the three permanent negative charges on the substituents. Interestingly, the basicity of the solvent is less important for the ESPT reaction. In contrast, all conjugated bases as the reaction products of ESPT are extremely weak bases in the excited state. A systematic relation to the chemical structure could not be unraveled for the latter.

Inspired by quantum-chemical computations, we could show that the energetic distance between the two lowest excited states is modulated by the substituents in the same direction as the photoacidity. Although being far away from a thorough understanding, the experimental findings including the vibronic progression will guide further elaborate calculations. Future research should also focus on higher electronic states and their dependence on the substituents.

Acknowledgements

We thank Volker Huch for help with the crystallographic structure. This work was supported by the German Science Foundation (DFG, JU650/3-1).

Notes and references

1 T. Förster, *Naturwissenschaften*, 1949, **36**, 186.
2 N. Agmon, *J. Phys. Chem. A*, 2005, **109**, 13.
3 J. T. Hynes, T. Tran-Thi and G. Granucci, *J. Photochem. Photobiol., A*, 2002, **154**, 3.
4 L. G. Arnaut and S. J. Formosinho, *J. Photochem. Photobiol., A*, 1993, **75**, 1.
5 E. Pines, in *The Chemistry of Phenols*, ed. Z. Rappoport, John Wiley & Sons, Ltd, 2003, pp. 491–527.
6 D. Pines and E. Pines, in *Hydrogen-Transfer Reactions*, ed. J. T. Hynes, J. P. Klinman, H.-H. Limbach and

R. L. Schowen, Wiley-VCH Verlag GmbH & Co. KGaA, Weinheim, 2007, pp. 377–415.
7 P. M. Kiefer and J. T. Hynes, in *Hydrogen-Transfer Reactions*, ed. J. T. Hynes, J. P. Klinman, H.-H. Limbach and R. L. Schowen, Wiley-VCH Verlag GmbH & Co. KGaA, Weinheim, 2006, pp. 303–348.
8 N. Agmon, W. Rettig and C. Groth, *J. Am. Chem. Soc.*, 2002, **124**, 1089.
9 L. N. Silverman, D. B. Spry, S. G. Boxer and M. D. Fayer, *J. Phys. Chem. A*, 2008, **112**, 10244.
10 D. B. Spry and M. D. Fayer, *J. Chem. Phys.*, 2007, **127**, 204501.
11 D. B. Spry and M. D. Fayer, *J. Chem. Phys.*, 2008, **128**, 084508.
12 O. F. Mohammed, J. Dreyer, B.-Z. Magnes, E. Pines and E. T. J. Nibbering, *ChemPhysChem*, 2005, **6**, 625.
13 T.-H. Tran-Thi, C. Prayer, P. Millié, P. Uznanski and J. T. Hynes, *J. Phys. Chem. A*, 2002, **106**, 2244.
14 A. Szemik-Hojniak, L. Wisniewski, I. Deperasinska, A. Makarewicz, L. Jerzykiewicz, A. Puszko, Y. Erez and D. Huppert, *Phys. Chem. Chem. Phys.*, 2012, **14**, 8147.
15 J. M. Paredes, L. Crovetto, A. Orte, J. Alvarez-Pez and E. M. Talavera, *Phys. Chem. Chem. Phys.*, 2011, **13**, 1685.
16 F. D. Lewis, L. E. Sinks, W. Weigel, M. C. Sajimon and E. M. Crompton, *J. Phys. Chem. A*, 2005, **109**, 2443.
17 A. A. Freitas, F. H. Quina and A. A. L. Maçanita, *J. Phys. Chem. A*, 2011, **115**, 10988.
18 E. Gould, A. V. Popov, L. M. Tolbert, I. Presiado, Y. Erez, D. Huppert and K. M. Solntsev, *Phys. Chem. Chem. Phys.*, 2012, **14**, 8964.
19 M. Mosquera, J. C. Penedo, M. C. Ríos Rodríguez and F. Rodríguez-Prieto, *J. Phys. Chem.*, 1996, **100**, 5398.
20 A. J. G. Strandjord, D. E. Smith and P. F. Barbara, *J. Phys. Chem.*, 1985, **89**, 2362.
21 B. Cohen, C. M. Álvarez, N. A. Carmona, J. A. Organero and A. Douhal, *J. Phys. Chem. B*, 2011, **115**, 7637.
22 Y. Erez, R. Gepshtein, I. Presiado, K. Trujillo, K. Kallio, S. J. Remington and D. Huppert, *J. Phys. Chem. B*, 2011, **115**, 11776.
23 K. M. Solntsev and N. Agmon, *Chem. Phys. Lett.*, 2000, **320**, 262.
24 L. M. Tolbert and J. E. Haubrich, *J. Am. Chem. Soc.*, 1990, **112**, 8163.
25 S. G. Schulman, W. R. Vincent and W. J. M. Underberg, *J. Phys. Chem.*, 1981, **85**, 4068.
26 C. M. Harris and B. K. Selinger, *J. Phys. Chem.*, 1980, **84**, 891.
27 A. Weller, *Z. Elektrochem.*, 1952, **56**, 662.
28 D. Huppert, L. M. Tolbert and S. Linares-Samaniego, *J. Phys. Chem. A*, 1997, **101**, 4602.
29 S. Mahanta, B. K. Paul, R. Balia Singh and N. Guchhait, *J. Comput. Chem.*, 2011, **32**, 1.
30 S. G. Schulman, S. X. Chen, F. L. Bai, M. J. P. Leiner, L. Weis and O. S. Wolfbeis, *Anal. Chim. Acta*, 1995, **304**, 165.
31 D. B. Spry, A. Goun and M. D. Fayer, *J. Phys. Chem. A*, 2007, **111**, 230.
32 S. K. Mondal, S. Ghosh, K. Sahu, P. Sen and K. Bhattacharyya, *J. Chem. Sci.*, 2007, **119**, 71.
33 D. B. Spry, A. Goun, C. B. Bell III and M. D. Fayer, *J. Chem. Phys.*, 2006, **125**, 144514.
34 T.-H. Tran-Thi, T. Gustavsson, C. Prayer, S. Pommeret and J. T. Hynes, *Chem. Phys. Lett.*, 2000, **329**, 421.
35 D. B. Spry and M. D. Fayer, *J. Phys. Chem. B*, 2009, **113**, 10210.
36 P. Leiderman, R. Gepshtein, A. Uritski, L. Genosar and D. Huppert, *J. Phys. Chem. A*, 2006, **110**, 9039.
37 L. Genosar, B. Cohen and D. Huppert, *J. Phys. Chem. A*, 2000, **104**, 6689.
38 B. Cohen, J. Segal and D. Huppert, *J. Phys. Chem. A*, 2002, **106**, 7462.
39 T. Htun, *J. Fluoresc.*, 2003, **13**, 323.
40 S. Kaneko, S. Yotoriyama, H. Koda and S. Tobita, *J. Phys. Chem. A*, 2009, **113**, 3021.
41 L. M. Tolbert and K. M. Solntsev, *Acc. Chem. Res.*, 2002, **35**, 19.
42 R. Simkovitch, E. Kisin-Finfer, S. Shomer, R. Gepshtein, D. Shabat and D. Huppert, *J. Photochem. Photobiol., A*, 2013, **254**, 45.
43 L. M. Tolbert and J. E. Haubrich, *J. Am. Chem. Soc.*, 1994, **116**, 10593.
44 K. M. Solntsev, D. Huppert and N. Agmon, *J. Phys. Chem. A*, 1999, **103**, 6984.
45 K. M. Solntsev, D. Huppert, N. Agmon and L. M. Tolbert, *J. Phys. Chem. A*, 2000, **104**, 4658.
46 C. Clower, K. M. Solntsev, J. Kowalik, L. M. Tolbert and D. Huppert, *J. Phys. Chem. A*, 2002, **106**, 3114.
47 T. B. McAnaney, X. Shi, P. Abbyad, H. Jung, S. J. Remington and S. G. Boxer, *Biochemistry*, 2005, **44**, 8701.
48 F. Wong and C. Fradin, *J. Fluoresc.*, 2011, **21**, 299.
49 P. Leiderman, A. Uritski and D. Huppert, *J. Phys. Chem. A*, 2007, **111**, 4998.
50 K. Das, K. D. Ashby, J. Wen and J. W. Petrich, *J. Phys. Chem. B*, 1999, **103**, 1581.
51 B. Cohen and D. Huppert, *J. Phys. Chem. A*, 2000, **104**, 2663.
52 B. Cohen, P. Leiderman and D. Huppert, *J. Phys. Chem. A*, 2002, **106**, 11115.
53 A. Uritski, I. Presiado, Y. Erez, R. Gepshtein and D. Huppert, *J. Phys. Chem. C*, 2009, **113**, 17915.
54 L. Genosar, P. Leiderman, N. Koifman and D. Huppert, *J. Phys. Chem. A*, 2004, **108**, 1779.
55 R. Barnadas-Rodríguez and J. Estelrich, *J. Photochem. Photobiol., A*, 2008, **198**, 262.
56 P. Leiderman, R. Gepshtein, A. Uritski, L. Genosar and D. Huppert, *J. Phys. Chem. A*, 2006, **110**, 5573.
57 I. Presiado, Y. Erez, R. Gepshtein and D. Huppert, *J. Phys. Chem. C*, 2009, **113**, 20066.
58 A. Mirończyk and A. Jankowski, *J. Photochem. Photobiol., A*, 2002, **153**, 89.
59 J. Alvarez-Pez, L. Ballesteros, E. Talavera and J. Yguerabide, *J. Phys. Chem. A*, 2001, **105**, 6320.
60 K. M. Solntsev, D. Huppert and N. Agmon, *Phys. Rev. Lett.*, 2001, **86**, 3427.
61 E. Pines, D. Huppert and N. Agmon, *J. Chem. Phys.*, 1988, **88**, 5620.
62 N. Agmon, E. Pines and D. Huppert, *J. Chem. Phys.*, 1988, **88**, 5631.

63 N. Agmon, *J. Chem. Phys.*, 1988, **88**, 5639.
64 N. Agmon and I. V. Gopich, *Chem. Phys. Lett.*, 1999, **302**, 399.
65 P. Leiderman, L. Genosar and D. Huppert, *J. Phys. Chem. A*, 2005, **109**, 5965.
66 S. Park, Y. Lee and D. Jang, *Phys. Chem. Chem. Phys.*, 2008, **10**, 6703.
67 A. Melnichuk, *J. Chem. Phys.*, 2011, **134**, 244303.
68 W. Zhao, L. Pan, W. Bian and J. Wang, *ChemPhysChem*, 2008, **9**, 1593.
69 K. M. Solntsev, D. Huppert, L. M. Tolbert and N. Agmon, *J. Am. Chem. Soc.*, 1998, **120**, 7981.
70 K. M. Solntsev, D. Huppert and N. Agmon, *J. Phys. Chem. A*, 1998, **102**, 9599.
71 A. Bani-Yaseen, *J. Fluoresc.*, 2011, **21**, 1061.
72 R. S. Moog, D. D. Kim, J. J. Oberle and S. G. Ostrowski, *J. Phys. Chem. A*, 2004, **108**, 9294.
73 C. Reichardt, *Solvents and solvent effects in organic chemistry*, VCH, Weinheim, 1988.
74 E. Lippert, *Z. Elektrochem.*, 1957, **61**, 962.
75 N. Mataga, Y. Kaifu and M. Koizumi, *Bull. Chem. Soc. Jpn.*, 1956, **29**, 465.
76 W. Liptay, *Angew. Chem., Int. Ed. Engl.*, 1969, **8**, 177.
77 M. J. Kamlet, J. L. M. Abboud, M. H. Abraham and R. W. Taft, *J. Org. Chem.*, 1983, **48**, 2877.
78 J. Catalán, *J. Phys. Chem. B*, 2009, **113**, 5951.
79 B.-Z. Magnes, D. Pines, N. Strashnikova and E. Pines, *Solid State Ionics*, 2004, **168**, 225.
80 G. Jung, S. Gerharz and A. Schmitt, *Phys. Chem. Chem. Phys.*, 2009, **11**, 1416.
81 N. Barrash-Shiftan, B. Brauer and E. Pines, *J. Phys. Org. Chem.*, 1998, **11**, 743.
82 B. Finkler, C. Spies, M. Vester, F. Walte, K. Omlor, I. Riemann, M. Zimmer, F. Stracke, M. Gerhards and G. Jung, 2013, submitted.
83 E. Pines, D. Pines, Y. Z. Ma and G. R. Fleming, *ChemPhysChem*, 2004, **5**, 1315.
84 G. Angulo, G. Grampp and A. Rosspeintner, *Spectrochim. Acta, Part A*, 2006, **65**, 727.
85 S. A. Hennessy, S. D. McDermott and S. M. Moane, *J. Forensic Sci.*, 2004, **49**, 1.
86 C. Laurence, P. Nicolet, M. T. Dalati, J. M. Abboud and R. Notario, *J. Phys. Chem*, 1994, **98**, 5807.
87 Wavefunction, Inc., *Phys. Chem. Chem. Phys.*, 2006, **8**, 3172.
88 M. J. Frisch, G. W. Trucks, H. B. Schlegel, G. E. Scuseria, M. A. Robb, J. R. Cheeseman, G. Scalmani, V. Barone, B. Mennucci, G. A. Petersson, H. Nakatsuji, M. Caricato, X. Li, H. P. Hratchian, A. F. Izmaylov, J. Bloino, G. Zheng, J. L. Sonnenberg, M. Hada, M. Ehara, K. Toyota, R. Fukuda, J. Hasegawa, M. Ishida, T. Nakajima, Y. Honda, O. Kitao, H. Nakai, T. Vreven, J. A. Montgomery, J. E. Peralta, F. Ogliaro, M. Bearpark, J. J. Heyd, E. Brothers, K. N. Kudin, V. N. Staroverov, R. Kobayashi, J. Normand, K. Raghavachari, A. Rendell, J. C. Burant, S. S. Iyengar, J. Tomasi, M. Cossi, N. Rega, J. M. Millam, M. Klene, J. E. Knox, J. B. Cross, V. Bakken, C. Adamo, J. Jaramillo, R. Gomperts, R. E. Stratmann, O. Yazyev, A. J. Austin, R. Cammi, C. Pomelli, J. W. Ochterski, R. L. Martin, K. Morokuma, V. G. Zakrzewski, G. A. Voth, P. Salvador, J. J. Dannenberg, S. Dapprich, A. D. Daniels, Ö. Farkas, J. B. Foresman, J. V. Ortiz, J. Cioslowski and D. J. Fox, *Gaussian 09, Revision B.01*, Gaussian, Inc., Wallingford, CT, 2009.
89 T. Clark, A. Alex, B. Beck, F. Burkhardt, J. Chandrasekhar, P. Gedeck, A. Horn, M. Hutter, B. Martin, G. Rauhut, W. Sauer, T. Schindler and T. Steinke, *VAMP 10.0*, CCC, Erlangen, 2009.
90 A. M. Williams, Y. Jiang and D. Ben-Amotz, *Chem. Phys.*, 1994, **180**, 119.
91 R. Pappalardo and S. Ahmed, *J. Chem. Phys.*, 1972, **56**, 5135.
92 M. Lukeman, M. Burns and P. Wan, *Can. J. Chem.*, 2011, **89**, 433.
93 M. Drobizhev, S. Tillo, N. S. Makarov, T. E. Hughes and A. Rebane, *J. Phys. Chem. B*, 2009, **113**, 12860.
94 D. A. Horke, A. S. Chatterley and J. R. R. Verlet, *Phys. Rev. Lett.*, 2012, **108**, 083003.
95 A. Hakonen and S. Hulth, *Anal. Chim. Acta*, 2008, **606**, 63.
96 F. Messina, M. Prémont-Schwarz, O. Braem, D. Xiao, V. S. Batista, E. T. J. Nibbering and M. Chergui, *Angew. Chem., Int. Ed.*, 2013, **52**, 6871.